High-occupancy vehicle lanes: modeling the upstream interface capacity

Mathis Boukhellouf, Nicolas Chiabaut, Christine Buisson

High-occupancy vehicle lanes: modeling the upstream interface capacity

Mathis Boukhellouf*[1], Nicolas Chiabaut[2], and Christine Buisson[3]

[1]Ph. D. student, École nationale des travaux publics de l'État, LICIT-Éco7, France

[2]Ph. D., Citec Ingénieurs Conseils SAS, France

[3]Ph. D., Senior researcher, Université Gustave Eiffel, LICIT-Éco7, France

SHORT SUMMARY

This work contributes to the understanding of the behavior of the upstream end of a high-occupancy vehicle (HOV) lane. Indeed, just upstream of this lane, vehicles may change lanes to be sure they are allowed to use the downstream lane (either HOV or general-purpose lane(s)). This upstream end is therefore the place of lane changes that may reduce the capacity. To estimate this drop, we adapt an existing weaving section analytical model to this upstream interface. We assess this model by comparison with the maximal theoretical supply and with simulation results. Our model adaptation indeed reproduces a capacity drop. Although with a less important drop, simulation results are coherent, except for cases with 0 or 100% of the vehicles being highly occupied. Further work should focus on treating the successive lane changes when considering more than two upstream lanes, and on comparing the results with the ones of other simulators.

Keywords: capacity drop, high-occupancy vehicle lanes, microscopic traffic simulation, shared mobility, traffic flow theory, weaving section.

1. INTRODUCTION

Since the end of the 2010s, European public authorities, and particularly in France, have been moving more and more towards the deployment of high-occupancy vehicle (HOV) lanes (HLs) to regulate highway traffic. Opened in the United States since the 1970s on networks with bottlenecks, these lanes are only accessible to vehicles carrying people who share their mobility whether through carpooling or using public transport, and in some cases to low-emission vehicles. HLs being designed to be uncongested, one can reward people adopting a virtuous behavior towards car use with shorter travel times. Meanwhile, self-drivers remain in the congested general-purpose lanes (GLs). This type of planning is particularly deployed on roads leading to a central business district (CBD), as they are heavily traveled during workdays' peak periods. In the long term, the strategic objective is therefore to foster a modal shift towards cleaner mobility. However, it should first be ensured that in the short term, traffic conditions induced by the HL activation avoid the propagation of queues to upstream strategic nodes, as well as guaranteeing a convincing travel time differential between carpoolers and self-drivers.

In Europe, rather than building a new lane or marking permanently the road surface as is mostly the case in the United States, the leftmost lane on the highway is temporarily allocated to HOVs. A typical case is shown in figure 1, with an HL-section of length $\ell_{\mathscr{H}}$ leading to a downstream bottleneck whose supply is Ω. In this situation, (Menendez & Daganzo, 2007) and (Daganzo & Cassidy, 2008) give conditions on the flows of each type of lane so that the HL activation is not

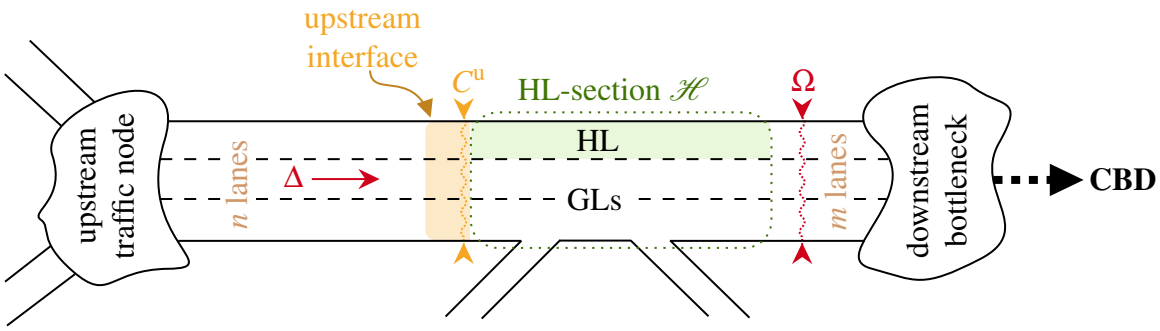

Figure 1: Depiction of a HL deployment project, showcasing the potential issues due to the network geometry

an active bottleneck. Assuming the theoretical capacity of one HL and one GL are the same and equal q_x,

$$\begin{cases} \forall x \in [0\,;\,\ell_{\mathscr{H}}],\ q_{\mathrm{H}}(x) \leq q_x \\ \forall x \in [0\,;\,\ell_{\mathscr{H}}],\ q_{\mathrm{G}}(x) \leq (n-1)q_x \\ q_{\mathrm{H}}(x=\ell_{\mathscr{H}}) \leq \Omega/m \end{cases} \tag{1}$$

The first two conditions reflect physical constraints, as the flows cannot overpass the capacity. It means that traffic conditions should be checked at any potential bottleneck (HL (de)activation, on- or off-ramp, lane drop, ...) so that if not met at any position in the section, congestion starts from this position. The last condition applies at the downstream end of the HL, assuming there are m downstream lanes. It is stronger than the first one because if not met, the HL is saturating from downstream, meaning that the deployment fails, as HOVs cannot gain travel time.

By adapting conditions (1), (Hans & Damas, 2019) and (Rousic et al., 2020) model the use domain of an HL-section. It ensures fluidity in the HL and congestion from downstream in the GLs so that the HL acts like a bottleneck for self-drivers. They assume that either there is no ramp or the inflows equal the outflows so that the flows arriving at the end of the section shall roughly be the same as the ones at $x = 0$. Thus, the conditions of this use domain focus on the upstream demands:

$$\begin{cases} \Delta \geq \Omega \\ (1-\alpha)\Delta \leq (n-1)q_x \\ \alpha\Delta \leq \Omega/m \end{cases} \tag{2}$$

α being the HOVs proportion. The first condition states that the section is congested, and the second one ensures the GLs should not saturate from upstream. The last condition is the same as (1), ensuring the HL does not saturate from downstream.

The main shortcoming of this framework is that it does not consider the phenomena occurring at the upstream and downstream interfaces, *i.e.* the way vehicles join their assigned lane and how they rearrange once the HL is deactivated, generating lane changes (LCs). The aggregation of these individual behaviors may induce a capacity drop (Leclercq et al., 2016), so that the two last conditions of (2), regarding the inflows at $x = 0$, should be modified due to the exogenous limitations of the capacities. Indeed, underestimating the possible drop upstream of the HL entrance leads to underestimating the increase in travel times and in queues length, which may then propagate up to sensitive traffic nodes. Thus, to make the use domain more reliable, this work investigates analytically and in simulation the HL upstream interface capacity.

2. METHODOLOGY

Our aim is to provide tools to better estimate the upstream capacity of sections where one of the downstream lanes is dedicated to HOVs. Table 1 presents all variables and parameters describing

Table 1: Variables and parameters used in the modeling

Variable/parameter	Notation	Value
HOVs proportion	α	
Upstream demand (all lanes)	Δ	
Number of upstream lanes	n	
Free-flow speed	u	19.44 m/s
Congestion wave maximum speed	w	5.4 m/s
Jam density (one lane)	κ	0.15 veh/m
Theoretical capacity (one lane)	q_x	2282 veh/h
Acceleration after changing lanes	a	3 m/s^2
Weaving vehicles proportion from lane i	β_i	
LCs zone length	L	1000 m
Upstream demand (lane i)	λ_i	
Effective flow (lane i)	q_i	
Upstream interface capacity (all lanes)	C^{u}	
Priority ratio in upstream general saturation	δ	

the upstream limit of an HL-section. The α ratio, corresponding to the HOVs proportion, as well as n, the number of upstream lanes, are the key factors for the operation of the upstream limit of those zones.

To reach our aim, for now, we rely on the tools available without experiment, because we want to make the estimation before the experimental deployment of HLs. Varying α from 0 to 1 and n from 2 to 3, we use three methods:

- first, a lower-bound capacity is derived, based on the endogenous capacity computed with a model inspired from the weaving sections,
- secondly, an upper-bound capacity (or theoretical supply) is defined, according to equation (1),
- thirdly, we use a microscopic tool to explore the simulation results for this configuration.

Lower-bound capacity estimation

As the movements upstream an HL-section are similar to the ones all along a weaving section (see figure 2), we consider the upstream interface to be a specific type of weaving section. Thus, to derive the capacity, we chose to adapt the findings of (Marczak et al., 2015)'s work. It explains how traffic operates on the highway discontinuity induced by the proximity between an on-ramp and an off-ramp and by the individual differences in the origin and the destination choice. A proportion β_i of the demand λ_i coming from lane i takes the off-ramp, while a proportion β_j of the demand λ_j coming from the on-ramp (lane j) joins lane i, see figure 2(a). Macroscopically, this weaving section is modeled as the superposition of two merges and two diverges, since on each lane vehicles are inserting (merging operation) and others are deserting (diverge operation). For each operation, individual behaviors are considered, such as acceleration after changing lane to reach the free-flow speed, or that LCs occur along a zone of a certain length and create voids, so that the capacity drop caused by weaving flows is endogenously derived. This formulation relies on an allocation scheme of the flows, following the Newell-Daganzo model (Newell, 1982; Daganzo, 1995), which returns three possible ways of allocating the capacity C on the two upstream lanes i and j, depending on the demands' level and distribution: (*i*) both lanes free flow ($q_i = \lambda_i$, $q_j = \lambda_j$); (*ii*) one lane saturates and the other free flows ($q_i = \lambda_i$, $q_j = C - \lambda_i$; or $q_i = C - \lambda_j$, $q_j = \lambda_j$); (*iii*)

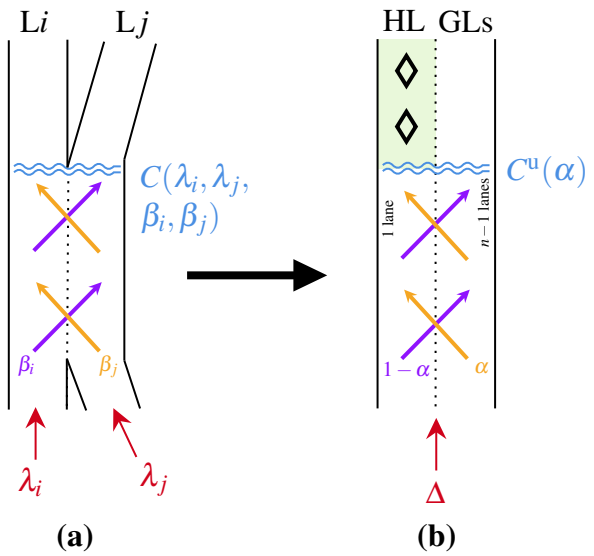

Figure 2: From the classic weaving section model (a) to the HL upstream interface weaving model (b)

both lanes saturate, the total effective flow being shared between both lanes with respect to a priority coefficient δ ($q_j/q_i = \delta$). Thus, effective flows are derived when at least one lane is congested. Assuming this lane is lane i, there are two possibilities to its macroscopic operation:

- *merge operation*: vehicles inserting from lane j worsen the traffic conditions on lane i. This operation lies on (Leclercq et al., 2016)'s merge model and derives effective flow q_i^{m},
- *diverge operation*: vehicles deserting from lane i worsen the traffic conditions on this lane by anticipating their change to lane j. This operation lies on (Laval, 2006, 2009)'s work and derives effective flow q_i^{d}.

The actual operation mode on lane i minimizes the effective flow, *i.e.* $q_i = \min(q_i^{\mathrm{m}}\ ;\ q_i^{\mathrm{d}})$. The weaving section capacity is then numerically derived – all calculation details are in (Marczak et al., 2015) – as $C(\lambda_i, \lambda_j, \beta_i, \beta_j) = q_i + q_j$.

However, some adaptations in Marczak's model should be done to take into account the specificities of HLs weave, assuming there is only one HL:

- we consider the two upstream lanes as two pipes of 1 lane (upstream of the HL) and $n-1$ lanes (upstream of the GLs), and assume the effective flows in general congestion are equally shared, *i.e.* $\delta = 1/(n-1)$,
- in Marczak's model, the LCs zone is strictly limited by the weaving section length. In its application to HLs, as there is no geometrical constraint, we make the strong assumption that LCs are possible all along a zone of length L upstream of the activation,
- as it is an exogenous parameter in the original model, macroscopic traffic relaxation is not considered,
- interestingly, the number of input parameters is reduced from four to one, as pictured in figure 2:
  - as vehicles come from the same origin, we can legitimately assume they are evenly distributed on the upstream lanes, *i.e.* $\lambda_{\mathrm{H}} = \Delta/n$ and $\lambda_{\mathrm{G}} = (n-1)\Delta/n$. Then, follow-

ing Newell-Daganzo's projection rule, only two traffic states are possible: fluidity or saturation on both upstream pipes. Thus, Δ is not a parameter anymore,

- as a consequence, HOVs are also uniformly distributed upstream. Since weaving flows depend on the HOVs proportion, we have $\beta_H = 1-\alpha$ and $\beta_G = \alpha$.

The adapted model then derives lower-bound capacity $C^u(\alpha)$, which matches with solid lines in figure 3.

Upper-bound capacity derivation

The upper-bound capacity coincides with the theoretical case without a capacity drop. It is derived depending on which type of lane is limiting due to a too important demand of self-drivers for the GLs ($(1-\alpha)\Delta \geq (n-1)q_x$), or of HOVs for the HL ($\alpha\Delta \geq q_x$). It thus equals $\min\left(\frac{(n-1)q_x}{1-\alpha}\ ;\ q_x/\alpha\right)$ and matches with dashed lines in figure 3.

Simulation framework

Simulations were performed with the microscopic traffic tool Aimsun (Aimsun, 2021), with calibrated fundamental diagram parameters matching with the values of (u, w, κ) in table 1. Varying α from 0 to 1 and inflowing an upstream demand of nq_x, effective flows are collected 250 meters downstream of the HL activation, to be sure vehicles reached the free-flow speed. To be statistically relevant due to the simulations stochasticity, 15 one-hour-simulations are considered, for each value of α. To elapse a potential warm-up phase, the flows collection holds for the 15 last simulated minutes. The simulated datasets match with the boxplots in figure 3, white dots representing the mean flow.

It is important to note that 11 replications, representing 3.33% of the total, lead to a complete gridlock before the end of the simulated hour. This is because of a vehicle arriving at the interface upstream of the wrong lane, and unable to change lanes due to the presence of another one arriving upstream of the wrong lane too, at exactly the same time instant. Those cases were discarded and replaced by new ones that do not present this problem.

3. RESULTS AND DISCUSSION

Figure 3 first compares the lower- and upper-bounds. It shows that our analytical formulation indeed integrates a capacity drop. Moreover, it exhibits the same variations as the theoretical supply, even if in the case the GLs are limiting, the capacity increase is less significant. It is also worth noting that for $n = 3$, the proportion maximizing the capacity is less than $1/3$, the theoretical one. It means that weaving flows start worsening the traffic conditions for lower HOVs proportions than when they are not considered. As a consequence, as shown in figure 4, the capacity drop, defined as the complement of the ratio between the lower- and the upper-bound, is more significant for $n = 3$. Indeed, an additional lane is affected by the weaving phenomena, generating more traffic instabilities induced by insertions or desertions.

When it comes to simulation results, we notice that for both numbers of lanes, simulated flows fall between the lower- and the upper-bounds, corroborating our model is realistic. Flows simulated for proportions near to the one maximizing the capacity are even close to the lower-bound ones. However, the closer we get to the borderline cases $\alpha \in \{0, 1\}$, the less capacity drop there is. When $\alpha = 0$ (resp. $\alpha = 1$), *i.e.* there is no carpooler (resp. no self-driver), the interface is a $1+(n-1)$-to-$n-1$ lanes (resp. $1+(n-1)$-to-1 lane) merge. Nonetheless, for $n = 2$, the drop has been

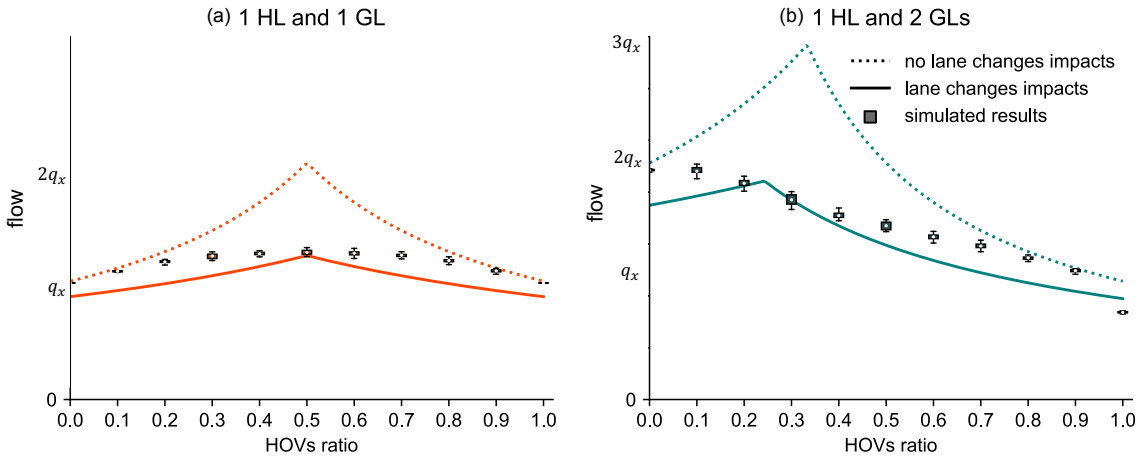

Figure 3: Upstream interface capacity derivation: comparing the theoretical supply with our model and with simulation results for two upstream lanes (a) and three upstream lanes (b)

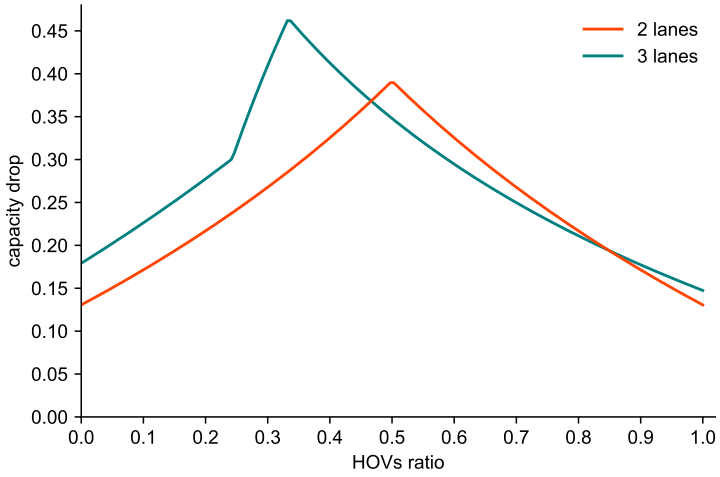

Figure 4: Capacity drop induced by the analytical modeling, for two and three upstream lanes

reported when using the same simulation configuration for an extended merge (Boukhellouf et al., 2022), making the upstream interface simulation results surprising. Another surprising result is the simulated borderline cases of $n = 3$, as we observe a drop for $\alpha = 1$ but not for $\alpha = 0$. This means that the $1+2$-to-1 lane merge induces a capacity drop but not the lane drop $1+2$-to-2 lanes one, because of a more important volume getting through a smaller bottleneck.

4. CONCLUSIONS

To fill the gap in the HLs upstream interface modeling, we proposed here to adapt an analytical model based on a weaving section operation. This adaptation is of flexible use, as the HOVs proportion is the only parameter. It integrates a capacity drop and gives consistent results so that the upstream interface is indeed a type of weaving section. However, when it comes to validation, Aimsun's results do not present a capacity drop when reaching high or low values of HOVs proportions. Thus, additional parameters of this tool, as LCs related ones, should be changed, or another simulator should be tested to validate the model. Finally, to improve the model, multilane merges (Marczak et al., 2016) should be considered to take into account more precisely the impact of HOVs successive LCs upstream of the GLs on the capacity drop.

REFERENCES

Aimsun. (2021). Aimsun next 20 user's manual (Aimsun Next 20.0.3 ed.) [Computer software manual]. Barcelona (Spain).

Boukhellouf, M., Buisson, C., & Chiabaut, N. (2022). Merging and diverging operations: benchmark of three European microscopic simulation tools and comparison with analytical formulations.
(Submitted to *European Transport Research Review*)

Daganzo, C. F. (1995). The cell transmission model, part II: Network traffic. *Transportation Research Part B: Methodological*, *29*(2), 79–93. doi: 10.1016/0191-2615(94)00022-R

Daganzo, C. F., & Cassidy, M. J. (2008). Effects of high occupancy vehicle lanes on freeway congestion. *Transportation Research Part B: Methodological*, *42*(10), 861–872. doi: 10.1016/j.trb.2008.03.002

Hans, É., & Damas, C. (2019). *Évaluation* a priori *des voies réservées au covoiturage sur voies structurantes d'agglomération* (Tech. Rep.). Lyon (France): Centre d'études et d'expertise sur les risques, l'environnement, la mobilité et l'aménagement. Retrieved from http://www.cerema.fr/system/files/documents/2019/05/guide_vsa_evaluation_a_priori_des_voies_reservees_au_covoiturage-mai_2019.pdf

Laval, J. A. (2006). Stochastic Processes of Moving Bottlenecks: Approximate Formulas for Highway Capacity. *Transportation Research Record*, *1988*, 86–91. doi: 10.3141/1988-13

Laval, J. A. (2009). Effects of geometric design on freeway capacity: Impacts of truck lane restrictions. *Transportation Research Part B: Methodological*, *43*(6), 720–728. doi: 10.1016/j.trb.2009.01.003

Leclercq, L., Knoop, V. L., Marczak, F., & Hoogendoorn, S. P. (2016). Capacity drops at merges: New analytical investigations. *Transportation Research Part C: Emerging Technologies*, *62*, 171–181. doi: 10.1016/j.trc.2015.06.025

Marczak, F., Leclercq, L., & Buisson, C. (2015). A Macroscopic Model for Freeway Weaving Sections. *Computer-Aided Civil and Infrastructure Engineering*, *30*, 13. doi: 10.1111/mice.12119

Marczak, F., Leclercq, L., Knoop, V., & Hoogendoorn, S. (2016). Capacity drops at merges: Analytical expressions for multilane freeways. In *Transportation Research Board 95th annual meeting.* Transportation Research Board. doi: 10.3141/2560-01

Menendez, M., & Daganzo, C. F. (2007). Effects of HOV lanes on freeway bottlenecks. *Transportation Research Part B: Methodological*, *41*(8), 809–822. doi: 10.1016/j.trb.2007.03.001

Newell, C. (1982). *Applications of Queueing Theory*. Chapman and Hall. doi: 10.1007/978-94-009-5970-5

Rousic, S., Ancelet, O., Levilly, B., & de Wissocq, M. (2020). *Voies structurantes d'agglomération. Aménagement des voies réservées au covoiturage et à certaines catégories de véhicules* (Tech. Rep.). Bron (France): Centre d'études et d'expertise sur les risques, l'environnement, la mobilité et l'aménagement.